URSI - RCRS 2022, IIT (Indore), India, 1 - 4 December, 2022

Performance evaluation of IRI, IRI-Plas and SAMI2 during the consecutive prolonged solar minimum of cycles 23 and 24 around 100°E

Angkita Hazarika* (1), Kalyan Bhuyan(1), Bitap R. Kalita(1) and Pradip K. Bhuyan(1)
(1) Dibrugarh University, India, 786004

Abstract

We have examined the performance of the International Reference Ionosphere (IRI 2016), International Reference Ionosphere extended to Plasmasphere (IRI-Plas 2017), and SAMI2 is Another Model of the Ionosphere (SAMI2) models under solar minimum quiet time period around 100°E by comparing with the total electron content (TEC) obtained from a chain of Global Navigation Satellite Systems receivers. The results show that all the models overestimate the observed TEC for all stations and seasons, with the highest overestimation observed for IRI Plas. The IRI 2016 model performed better for all stations and seasons than IRI Plas. IRI Plas 2017 model is also simulated by assimilating the TEC derived from GPS (GPS-TEC) and Global Ionospheric Map (GIM-TEC) into the model code. The "no input" option of the model is used as a reference to study the effect of data assimilation on the model's efficacy. It is observed that the assimilation of GPS TEC and GIM-TEC into the model code reproduces TEC quite well for all the quiet days considered during both solar minima. IRI-Plas and IRI 2016 simulation is also compared with SAMI2 simulations for the same space-time configuration. SAMI2 also overestimates the quiet time observed TEC during daytime peak hours in all northern and southern stations. Based on observed results, changes are made to the SAMI2 model inputs. By changing the ionizing EUV, neutral thermospheric composition, and neutral temperature, a good agreement between the simulated and measured data is obtained. However, due to strong tidal effects during low solar activity, additional modifications may be needed to the neutral density, temperature, and EUV. The drift model used in SAMI2 should also be replaced or modified for the low solar activity periods.

1. Introduction

The solar minimum between cycles 23 and 24 has been an unusual period of low solar activity, which was a record low and unusually prolonged (2006–2009). Solar activity continually decreased throughout 2007 and 2008 [1] though the minimum was expected to occur in 2006. The deficient solar activity is reflected as lower values in the solar fluxes (UV, EUV, and X-rays) and in the solar activity indices F10.7 and sunspot number compared to normal solar minima [2,3,4]. It was reported that the extreme solar ultraviolet (EUV) irradiance was approximately 15% lower than the previous solar minimum [5]. The thermosphere contracted to record low levels causing a decrease in density (at 400 km altitude) by about 30% due to the reduction of EUV irradiance [6,7]. The ionosphere also contracted to a thin shell, with the O^+/H^+ transition height and ion temperature reaching record low values as observed and modeled [8,9,10]. International Reference Ionosphere (IRI-2007) model overestimated the F region peak electron density (Nmax) than those observed by Champ and Grace satellites in 2008-2009 [11]. Similar differences are found while comparing IRI-2007 simulations with Communication/Navigation Outage Forecasting System (C/NOFS) observations. Global values of GPS-TEC and F region critical frequency (foF2) reached lower values than the previous minimum [12,13] However, mid-latitude observations suggest that the decrease in TEC was modest, and in some cases, N_{max} was even larger in 2008-2009 than those observed in the previous solar minimum [13] (Araujo-Pradere et al., 2011). The effects of tides and waves originating in the lower atmosphere were strong in the thermosphere and ionosphere during deep solar minimum. Due to the effects of semidiurnal tides, a complicated change in plasma drift and the neutral wind was also present during this period [13,14,15]. Thus, observations so far indicate that the low latitude ionosphere showed significant changes during the long deep solar minimum. Longitudinal variations were also noticed during this deep solar minimum period.

The strongest maxima of the global longitudinal WN4 structure in EIA, EEJ, density, TEC and vertical drift etc [16,17,18] are reported from 90°-100°E longitude. The low latitude region in this longitude sector is, therefore, dynamically different and challenging compared to any other longitude sector, as reported by previous researchers [19,20]. Bhuyan and Hazarika [19] studied the temporal variation of TEC over Dibrugarh (27.5°N, 95°E) during the ascending phase of solar cycle 24 from the solar minimum year of 2009 and compared the observed TEC with TEC predicted by International Reference Ionosphere (IRI-2012). They found that during the low solar activity year 2009, IRI underestimated the TEC over Dibrugarh in about all months and local times. A detailed modeling study is required to understand the role of different physical processes around this longitude sector during deep solar minimum. Again, the deficient solar activity during the solar cycle 24/23 provides an opportunity to check the reliability of physical ionospheric models in 95°-100°E longitude sector.

In this study, we test the prediction efficiencies of the International Reference Ionosphere (IRI 2016), International Reference Ionosphere extended to Plasmasphere (IRI-Plas 2017), and SAMI2 is Another Model of the Ionosphere (SAMI2) models under solar minimum quiet time period around 100° E by comparing with the total electron content (TEC) obtained from a chain of Global Navigation Satellite Systems receivers. We also compare the model results observed in deep solar minimum 2009-2010 with those observed in recent solar minimum 2018-2019. The main objectives of this paper are 1) to examine the performance of IRI 2016, IRI Plas, and SAMI2 models in VTEC representation during the prolonged solar minimum, 2) to examine the IRI Plas 2017 model performance with GPS TEC and GIM TEC assimilation for prolonged solar minimum and 3) to modify the SAMI2 model according to the geophysical condition observed during the prolonged deep solar minimum period. This study's primary focus is to identify the limitations of empirical and physical models for further improvements during deep solar minimum.

2. Data and Methodology

The TEC data for Dibrugarh (27.5ºN, 95ºE, 43ºdip) is measured using a NOVATEL dual frequency GPS TEC and scintillation receiver (GSV 4004B) for 2009-2010. In addition, data from the International GPS Service (IGS) at Kunming (25.02ºN, 102.7ºE, 38º dip), Havelock Island (12.02ºN, 92.98ºE, 11º dip), Port Blair (12.02ºN, 92.98ºE, 11º dip) and Cocos Islands (12.2ºS, 96.8ºE, 43º dip) are utilized in this study. For 2018-2019, TEC data for Dibrugarh and Aizawl (23.7ºN, 92.8ºE, 36º dip) are used from NovAtel GPSTATION-6 GNSS Receiver.

Figure 1 shows the map of considered stations for this study. Aizawl, Dibrugarh, and Kunming are northern low latitude stations, whereas Cocos Islands is at a magnetically conjugate location to Dibrugarh. Havelock Island and Port Blair are the equatorial stations used for this study.

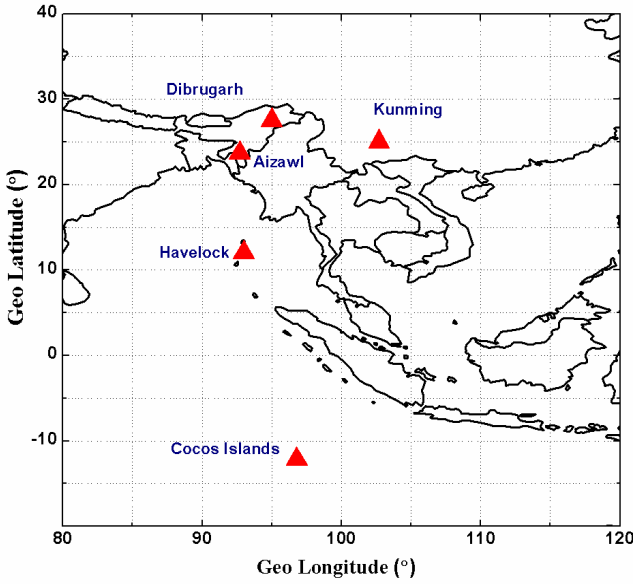

Figure 1. The map showing the locations of the ionospheric stations.

GPS Service (IGS) stations at Havelock Island, Kunming, and Cocos Islands is obtained from (ftp://cddis.gsfc.nasa.gov/pub/gps/data/-daily/) in RINEX format. RINEX files are converted to TEC using the GPS-TEC program [21] downloaded from http://seemala.blogspot. com/.

International Reference Ionosphere (IRI) is a standard empirical model sponsored by the Committee on Space Research (COSPAR) and International Union of Radio Science (URSI). The model is updated as new data become available and has been processed in the last two decades from IRI-2001. It is continuously updated and has many versions. Among them, IRI-2016 is the latest version of the IRI model used for this study. The most important and recent changes and improvements of this model version are described in detail by [22]. In this study, the CCIR model and NeQuick options for the topside profile estimation are considered. The default ABT-2009 option for the bottom-side thickness shape parameter is used.

IRI Extended to Plasmasphere (IRI-Plas) is a developed version of IRI model by Dr. Tamara L. Gulyaeva of IRI task group [23]. In IRI-Plas, it is possible to calculate VTEC up to the GPS satellite orbital height of 20,200 km. The plasmapheric density profile of IRI-Plas is provided by the Russian Standard Model for the ionosphere (SMI) plasmasphere model. The bottomside profile of the IRI-Plas model is the same with the IRI, because both models employed the CCIR or URSI map to calculate this section of the ionosphere [23]. However, the topside profile of the IRI-Plas model is improved using the topside sounder data from International Satellite for Ionospheric Studies (ISIS) 1, ISIS 2 and Russian Intercosmos –19 satellite (IK-19). For the plasmaspheric extension of the model, the topside density profile of IRI is fitted with the SMI plasmasphere model at an altitude of one basic scale height above the F2 layer peak height [24]. The basic scale height is above the F2 layer peak height, where the maximum electron density (NmF2) decays to NmF2*1/e, where e is the Euler number (~2.718). In addition to the plasmaspheric extension of the IRI-Plas model, the model algorithm can be adjusted with external data. The IRI-Plas algorithm allows the update of scale height by adjusting the model with external TEC data, thus providing the instantaneous value of the three key parameters (TEC, foF2 and hmF2) [25].

IRI-Plas is available as a FORTRAN code at ftp://ftp.izmiran.rssi.ru/pub/izmiran/SPIM/.In this investigation, the calculation of the modeled values is done using the online space weather services of the IONOLAB group and is available at www.ionolab.org. The online service uses the IRI-Plas software provided by the IZMIRAN Institute.

SAMI2 (Sami2 is Another Model of the Ionosphere) is a theoretical low-latitude ionospheric model [26]. It treats the dynamical and chemical evolution of the seven major ion species and electrons at altitudes starting at 90 km. SAMI2 provides densities, field-aligned drifts, and temperatures for each of the charged particle species as part of the standard output by solving the continuity and momentum equations for each of the ion species as well as for electrons. Thermal balance equations are also computed for H+, He+, O+, and the electrons. SAMI2 is the first low latitude ionospheric model to include the ion inertial terms in the momentum equations. The inclusion of ion inertia leads SAMI2 to simulate several new results like the formation of electron hole in the topside equatorial ionosphere, the formation of ion sound waves in the topside low latitude ionosphere etc [27].

3. Results and Discussions

In order to investigate the seasonal variations of TEC and to evaluate the IRI Plas, IRI 2016, and SAMI2 model performances around 100ºE, we consider March -April as the March equinox, May-August as the June solstice, September- October as the September equinox, and December-January as December Solstice depending on the availability of data.

We have simulated TEC using a number of IRI PLAS, IRI 2016 and SAMI2 simulations for selected quiet days of the study period around 100^0E longitude sector. The percentage deviation between model predictions and VTEC measurements is calculated as

$$\% D = \frac{(\text{Model prediction} - \text{Observed value})}{Observed\ Value} \times 100 \quad (1)$$

We have also calculated the Root Mean Square Deviation (RMSD) of the IRI-Plas, IRI2016 and SAMI2 from the GPS-TEC using Equations (3)

$$RMSD = \sqrt{\frac{\sum_1^n (X_{obs} - X_{model})^2}{n}} \quad (2)$$

where n is the number of data points, X_{obs} is the observed TEC Values, and X_{model} are the model values.

3.1. Comparison with IRI 2016, IRI PLAS 2017, and SAMI2 model simulation:

Fig.2 shows the percentage difference between the model and observed values for all seasons and stations during 2009-2010. In Fig.2 a positive %D value indicates that all models overestimate the observed TEC values, while a negative %D value indicates that the models underestimate the observed TEC; also, a zero or close to zero %D indicates more accurate predictions. We have also calculated the %D for recent solar minimum 2018-2019 for same space time conditions.

It is observed that IRI Plas highly overestimates the observed TEC for all stations and seasons for both solar minimum periods 2009-2010 and 2018-2019 than SAMI2 and IRI 2016.The bar charts in Fig.4 show the monthly averaged RMSD of TEC for IRI Plas, IRI 2016, and SAMI2 over all stations considered in solar minimum 2009 and 2018.

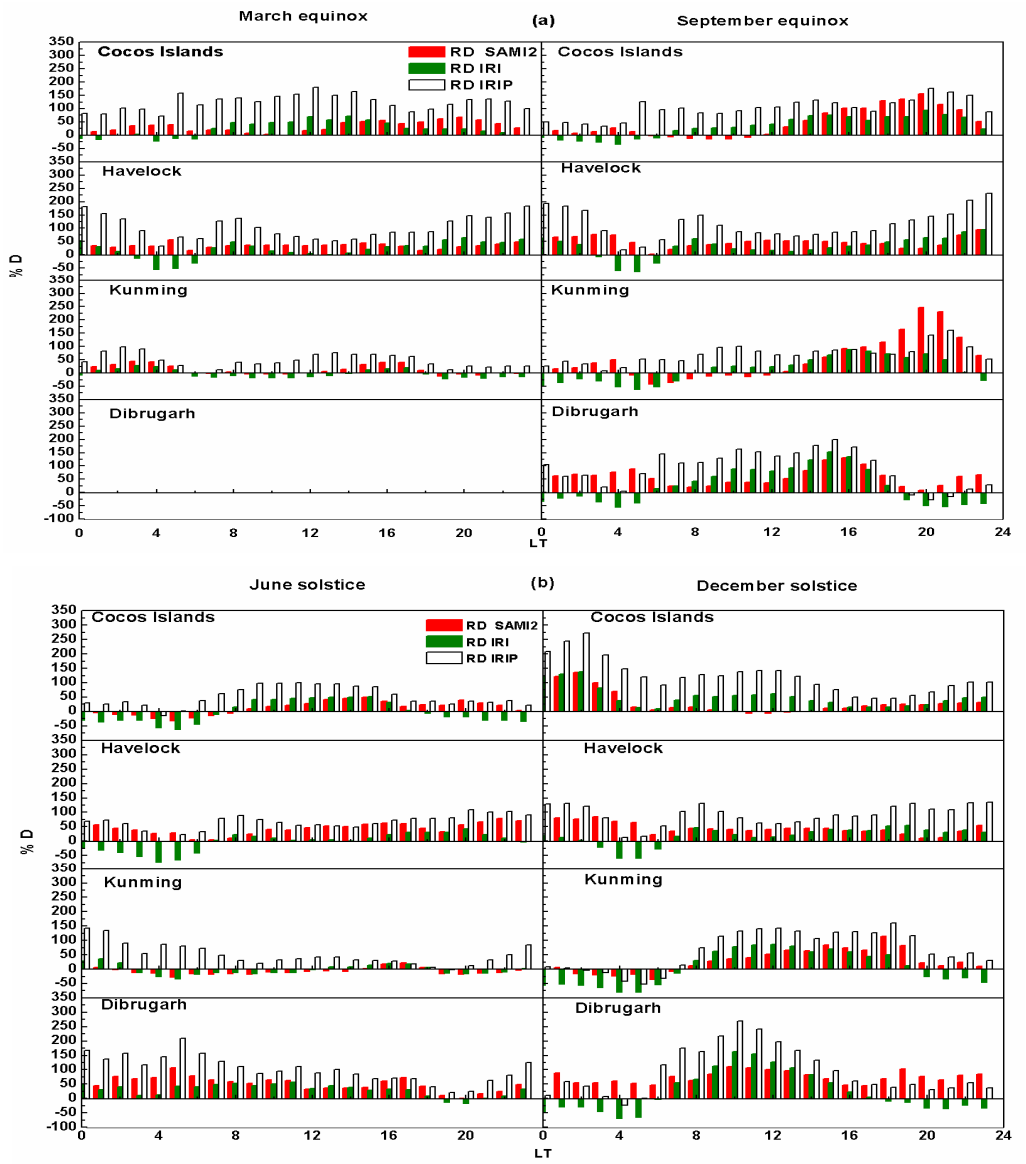

Figure 2. %D of modeled and observed VTEC for all stations and seasons for 2009-2010.

Thus, this section compares the prediction efficiency of IRI 2016, IRI Plas 2017 and SAMI2 models in VTEC representation during the deep solar minimum period 2009-2010 and recent solar minimum 2018-2019. All three models tend to overestimate the VTEC values mainly during daytime maximum ionization hours for all stations and seasons, with the highest overestimations observed for IRI Plas 2017. Of the two empirical models, IRI 2016 and IRI Plas 2017, IRI 2016 shows better performance (with RMSD less than 7 TECU) during both solar minima than IRI Plas. The overestimation observed by the models may be due to the inaccurate representation of the topside ionosphere due to inadequate estimation of the foF2 and hmF2 [28]. In addition, the inaccurate plasmaspheric VTEC estimation could result in the poor performance of the models in deep solar minimum. The larger IRI Plas VTEC values than IRI 2016 VTEC are due to the plasmaspheric VTEC contribution, which is included in the IRI Plas 2017 model up to 20000 km. However, the high overestimation observed for the IRI Plas model suggests that the plasmaspheric model used in IRI Plas needs further modification for deep solar minimums. Further, the overestimation observed by both empirical models IRI 2016 and IRI Plas 2017, may also be attributed to the lack of a representative database included in both models from a comparable deep solar minimum.

The physical model SAMI2 mostly overestimates the daytime TEC for stations and seasons during both solar minimum periods considered in this investigation (RMSD less than 7 TECU). Small underestimations are also observed for SAMI2 in some seasons and stations. It is also noted that SAMI2 also performs better than IRI Plas 2017. The limited performance observed for SAMI2 may be due to the lack of a representative dataset from a comparable solar minimum in the empirical models used

in SAMI2. Therefore, we should customize the model according to the geophysical conditions observed during these solar minimum periods to fully understand the mechanisms that cause the observed variability and quantify their effects

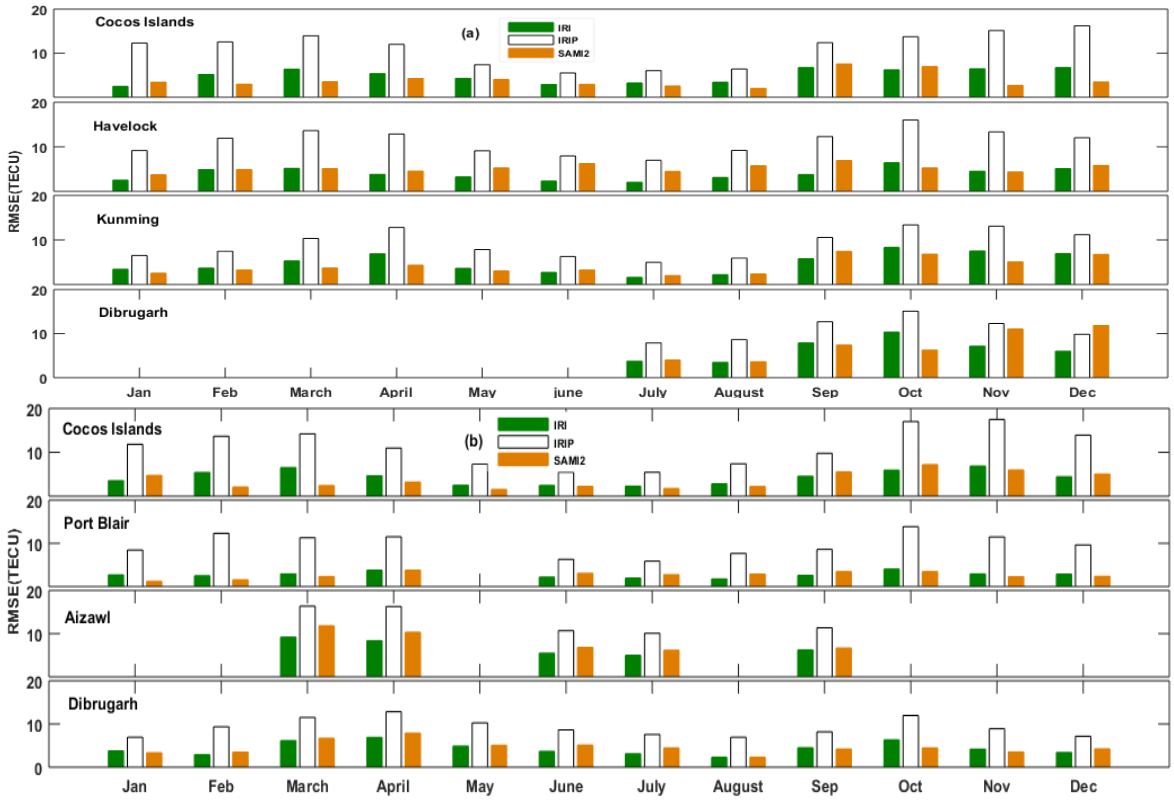

Figure 3. Monthly RMSDs for the year 2009 (a) and 2018 (b) for all the stations.

3.2. Comparison with IRI PLAS model simulation with assimilation of GPS and GIM TEC:

In this section, we simulated TEC using a number of IRI PLAS simulations for selected quiet days of the study period around 100^0E longitude sector using assimilation mode for same space time configuration. The model has been adjusted using the (i) GPS derived TEC (GPS-TEC) (ii) TEC derived from Global Ionospheric map (GIM). The GIM-TEC values available on the IONOLAB interface are used for our study. The no input option is used as a reference to evaluate the model's performance with TEC assimilation. It is observed that with GIM TEC and GPS TEC assimilation the model performs better than no input option. The percentage deviation is found lower for all stations and seasons with GIM and GPS TEC assimilation than no input option.

The bar charts in Fig.4 show the monthly averaged RMSD of TEC for IRI Plas with GIM TEC and GPS TEC assimilation over all stations considered in solar minimum 2009 and 2018. From figure.4 it is observed that with GPS TEC and GIM TEC assimilation, the performance of the IRI Plas model significantly improved for all months and stations during both solar minima. The RMSD is reduced to less than 4 TECU with GPS TEC assimilation and less than 6 TECU with GIM TEC assimilation in all months over all stations during both solar minima.

Thus, when the model is assimilated to TEC, better data-model agreement of TEC prediction is found over all stations and seasons for both solar minimum periods. Again, GPS TEC assimilation shows better results for all stations and seasons than GIM TEC assimilation mode. In the IRI PLAS model, TEC is calculated by integration of electron density profile between the path lengths 80-20000 km. Therefore, the model's performance in predicting TEC depends on its ability to reproduce the electron density profile [29]. The smaller values of model deviation when the model is assimilated to GPS and GIM TEC may be attributed to the improvement in rescaling of the topside profile due to the ingestion of external TEC into the model. The model exhibits better performance with GPS TEC assimilation than GIM TEC. It may be attributed to the error due to the complex spatial interpolation routine in estimating TEC in the GIM cell. Again, the shortcomings observed with GPS TEC

assimilation may be attributed to the uncertainty introduced due to modeling, calculation, and measurement errors in the parameters used as model inputs.

We have also studied the vertical density profile simulated by the IRI Plas model with no input and GPS TEC assimilation mode over Cocos during equinoxes for both solar minimum periods. It reveals that with GPS TEC assimilation, the density profile simulated by IRI Plas are modified for both solar minimum periods over Cocos. Thus, the better data model agreement

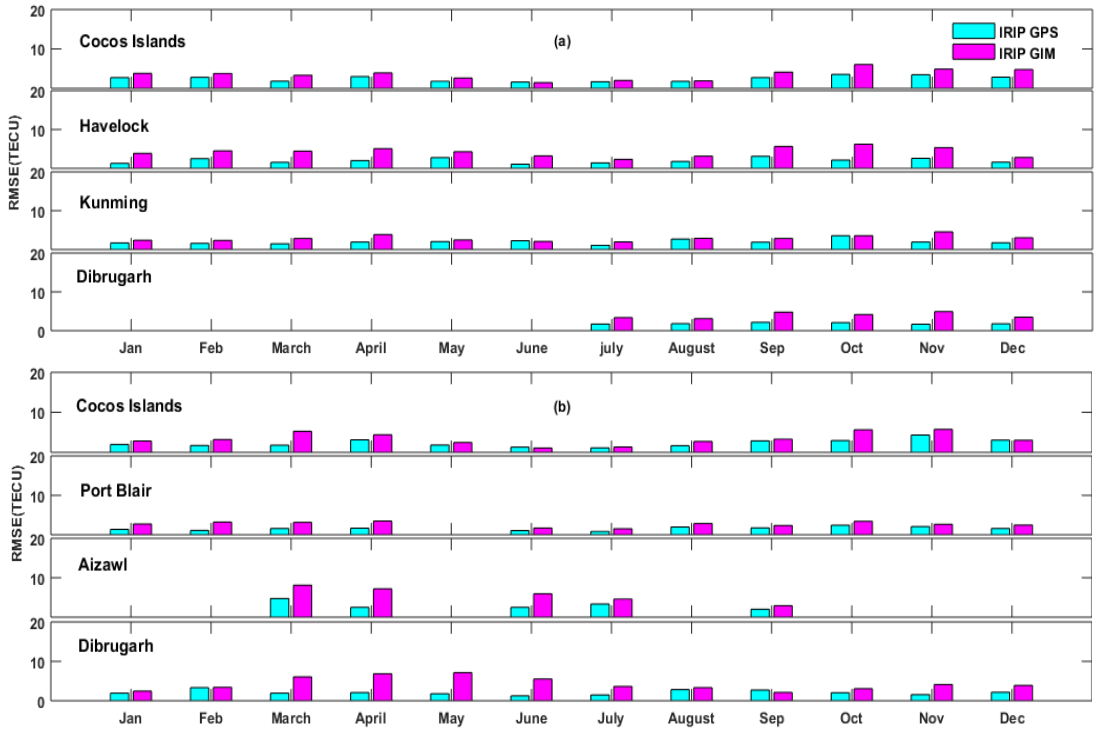

Figure 4. Monthly IRI Plas RMSD for the year 2009 (a) and 2018 (b) for all the stations with assimilation mode.

of TEC prediction with GPS TEC assimilation in the IRI PLAS model may be due to the improvement in rescaling the density profile.

3.3. Comparison with modified SAMI2 model simulation:

In this section, we customize the SAMI2 model according to the geophysical conditions observed during these deep solar minimum periods to fully understand the mechanisms that cause the observed variability and quantify their effects. To investigate the relative contributions of neutral density, neutral temperature and ionizing EUV to the observed results, changes are made to these model components for deep solar minimums. No changes are made in the wind model used in SAMI2.

3.2.1a. Neutral Density and Neutral temperature:
In SAMI2 neutral density and temperature are taken NRLMSISE-00 model (MSIS) [30]. It was reported that MSIS could not correctly predict the contracted neutral mass density observed during the extreme solar minimum [6] .To assess the ionospheric changes introduced by a contracted ionosphere, preliminary scaling factors for the exospheric temperature ($T_{\alpha scl}$ = 0.9603), neutral oxygen (Oscl = 0.7979), and other neutral species (n_{xscl} = 0.9697) are used [6,31] which were obtained by fitting the thermospheric mass density anomalies to measurements obtained by satellite drag calculations.

3.2.2b. Ionizing EUV:
In SAMI2 EUVAC model [32] provides EUV fluxes in 37 wavelength bins between 5 and 105 nm based on the solar radio flux at 10.7 cm (F10.7). As reported from the previous studies, we have reduced the EUV wavelengths in the EUVAC model by 15% [7,31].

It is noticed that %D shows low values with modified EUV and modified thermospheric composition and temperature for most of the time over all stations and seasons during solar minimum periods. It is also observed that with scaled MSIS, SAMI2

performs better than modified EUV during both equinoxes. With modified EUV and density, the %D decreases when overestimation is observed. However, %D increases for SAMI2 when underestimation is observed during both equinoxes.

The bar charts in figure.5 show the monthly averaged RMSD of TEC for SAMI2 with modified EUV and modified thermospheric density and Temperature over all stations considered in solar minimum 2009 and 2018. From the figure5. it is observed that with modified EUV and modified thermospheric composition and temperature, the RMSD decreases (less than 5 TECU) for SAMI2 for all months and stations during 2009. During 2018 we have also observed low values of RMSD for most of the months and stations, which indicate improvement of SAMI2 after modification during both solar minimums. To see the effect of modification in SAMI2 on Nmf2, we have aslso studied the diurnal variation of Nmf2 with modified SAMI2 simulations during equinoxes over Cocos, Havelock and Kunming for 2009-2010. It is noticed that lower value of Nmf2 is simulated by SAMI2 over all stations after modification. It is also noticed that the modification in EUV and MSIS also modified the vertical profile simulated by SAMI2 during deep solar minimum 2009-2010.

Lean et al.) [33] proposed that the SEM behavior does not represent exact solar EUV irradiance changes in 2008 relative to 1996 and the anomalously low thermospheric densities in 2008 are not directly solar driven. Our study also noticed that the effect of reduced neutral density and low EUV fluxes on the observed TEC is weak. There is also evidence that during the extreme solar minimum the effect of the tides on the ionosphere is stronger [34]. It is expected that the tidal effects in the troposphere may modify the neutral density, which in turn will modify the resultant ionosphere [35]. Additional modifications may be needed to the neutral density and temperature due to strong tidal effects during low solar activity. Neutral wind may also play an additional role in the observed TEC though we are not considering any modification in the HWM93 model used in SAMI2. There may be variation in the neutral winds as the effects of non-migrating tides are not included in the HWM93 model.

The drift model used in SAMI2 is Scherliess-Fejer (SF) model, which is based on the data from Atmospheric Explorer-E (AE-E) satellite and incoherent scatter radar at the Jicamarca Radio Observatory (JRO). Stoneback et al. [15] studied the local time distribution of meridional (vertical) drifts observed by the CINDI sensors on the C/NOFS spacecraft during the prolonged solar minimum dividing the globe into 60-degree longitude sectors. They reported the presence of a semidiurnal component in measured ion drifts, characterized by downward drift in the early afternoon and upward drift during the night. Downward

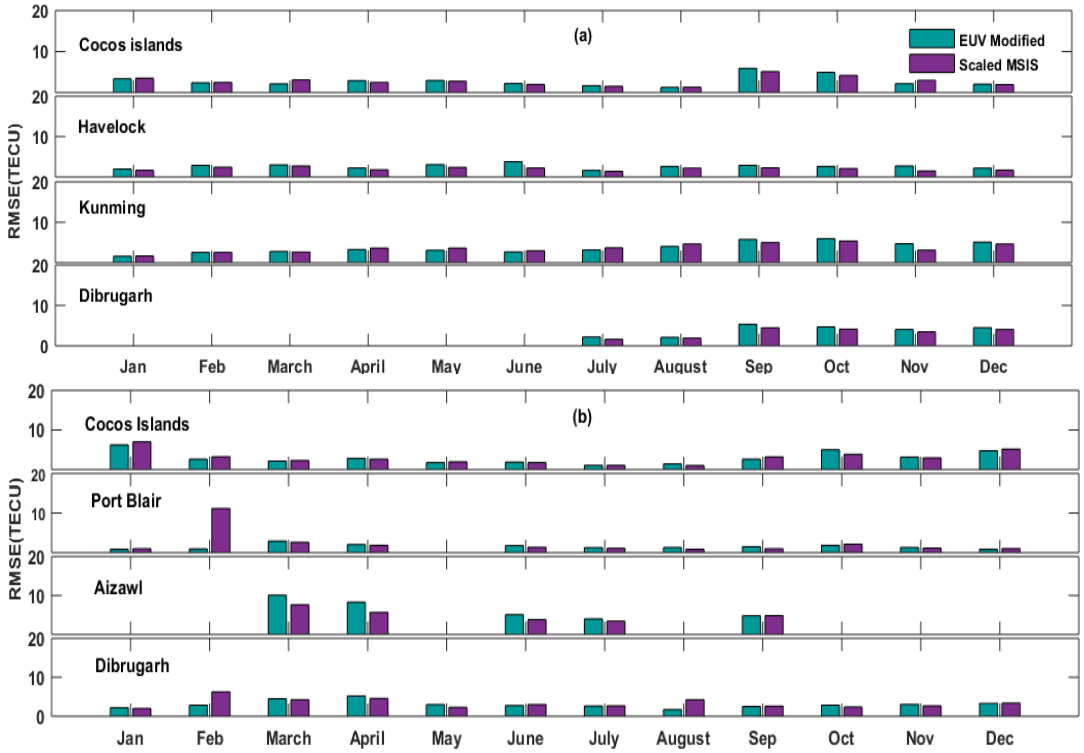

Figure 5. Monthly SAMI2 RMSD for the year 2009 (a) and 2018 (b) for all the stations with modification.

afternoon drifts were observed in all seasons almost over all longitudes, which were inconsistent with SF modeled drift. The average ExB drifts were again found to be different from the expected climatology during this deep solar minimum as measured by the Vector Electric Field Instrument (VEFI) on the C/NOFS satellite including downward drifts in the early afternoon and

a weak or nonexistent pre-reversal enhancement [31]. The SF model was reported to fail to simulate the differences observed in ExB drift during this period [31].

We have plotted the seasonal/diurnal pattern of the SF model simulated average vertical ExB drift for 90-110^0 E longitude sectors for 2009-2010. From the plot it is revealed that modeled drifts do not move downward until 20 LT during equinoxes, while during June and December solstices, the modeled drifts move downward at 18LT. In contrast to the modeled results, the past literature reported downward drifts in the early afternoon during this deep solar minimum. The model simulates a weak post sunset enhancement during both equinoxes and no postsunset enhancement during both solstices. SAMI2 may fail to simulate the observed contracted EIA during the deep solar minimum. Thus, the absence of large upward drift during the day or prereversal enhancement during the extreme solar minimum may play an essential role in the observed TEC. The increase in semidiurnal tide in the E region is also reported to affect the observed vertical drift during this period [15].

It is also observed that SAMI2 performs similarly for both solar minimum periods except for the northern stations. The absence of a strong plasma fountain [11] during solar minimum may play an essential role in the deviations of the observed TEC. Thus, the drift model, along with the other empirical models for neutral density and temperature, neutral wind, and solar EUV used in SAMI2, may not be able to predict the ionospheric conditions correctly during solar minimum.

4. Summary and conclusions:

In this study, we have analyzed the prediction efficiency of the ionospheric models IRI 2016, IRI PLAS 2017, and SAMI2 during the deep solar minimum quiet time period. The IRI-PLAS data is also generated by assimilating the TEC derived from GPS (GPS-TEC) and Global Ionospheric Map (GIM-TEC) into the model code. Depending on the observed results, we have modified the empirical models used in SAMI2 for low solar activity. The results are summarized as follows,

All three models overestimate the observed TEC during both low solar activity periods, with the highest overestimation observed for IRI Plas. It is also observed that IRI 2016 performs better than IRI Plas for all seasons and stations during the deep solar minimum periods. It indicates that the plasmaspheric model used in IRI Plas may need further modification.

The assimilation of GPS TEC and GIM TEC into the IRI Plas model significantly improves the model performance.

SAMI2 also overestimates the observed TEC most of the time during the low solar activity periods. The model agrees well with observed results with modified EUV and modified thermospheric composition and temperature. However, due to strong tidal effects during low solar activity, additional modifications may be needed to the neutral density, temperature, and EUV. The drift model used in SAMI2 should also be replaced or modified for the low solar activity period.

5. Acknowledgements

The authors would like to thank Dr. J. Huba for using the SAMI2 model ionospheric which was written and developed in the Naval Research Laboratory. The authors thank the IONOLAB group for making the IONOLAB-TEC and IRI Plas model available to the public through their online interface services available at http://www.ionolab.org The authors are also thankful to the International GNSS Service (IGS) for the GPS data and Dr. Gopi Seemala for the GPS-TEC analysis program used in this work. The authors acknowledge Mizoram University for the GNSS receiver infrastructure support.

7. References

1. C. T. Russell, J. G. Luhmann, and L. K. Jian., "How unprecedented a solar minimum?," *Reviews of Geophys*,**48**, 4, june 2010, doi:10.1029/2009RG000316.

2. N. Balan, G. J. Bailey and B. Jayachandran , "Ionospheric evidence for a non-linear relationship between the solar EUV and 10.7 cm fluxes during an intense solar cycle," *Planetary and Space Science*, **41**, 2, February 1993, pp. 141-145, doi:10.1016/0032-0633(93)90043-2.

3. D. L. Judge, D.R McMullin, H.S Ogawa, D. Hovestadt, B. Klecker, M. Hilchenbach, E. Möbius, L.R. Canfield, R.E. Vest, R. Watts, C. Tarrio, M. Kühne, and P. Wurz, "First solar EUV irradiances obtained from SOHO by the CELIAS/SEM," *Solar Physics*, **177**, January 1993, pp. 161-173, doi: 10.1023/A:1004929011427.

4. Y.Chen, L. Liu, and W. Wan, "Does the F10.7 index correctly describe solar EUV flux during the deep solar minimum of 2007–2009?," *Journal of Geophysical Research*, **116**, 4, March 2011, pp. 148-227, doi: 10.1029/2010JA016301.

5. S. C. Solomon, L. Qian, and A. G. Burns, "The anomalous ionosphere between solar cycles 23 and 24," *Journal of Geophysical Research*, **118**, 10, September 2013, pp. 6524–6535, doi: 10.1002/jgra.50561.

6. J. T.Emmert, J. L. Lean, and J. M. Picone, "Record-low thermospheric density during the 2008 solar minimum," *Geophysical Research Letters*, **37**, 12, June 2010, pp. L12102, doi: 10.1029/2010GL043671.

7. S. C. Solomon, L. Qian, L. V. Diskovsky, R. A. Viereck, and T. N. Woods, "Causes of low thermospheric density during 2007–2009 solar minimum," *Journal of Geophysical Research*, **116**, 2, February 2011, pp. A00H07, doi: 10.1029/2011JA016508.

8. R. A. Heelis, W. R. Coley, A. G. Burrell, M. R. Hairston, G. D. Earle, M. D. Perdue, R. A. Power, L. L. Harmon, B. J. Holt, and C. R. Lippincott, "Behavior of the O+/H+ transition height during the extreme solar minimum of 2008," *Geophysical Research Letters*, **36**, 18, July 2009, pp. L00C03, doi: 10.1029/ 2009GL038652.

9. N. Balan, C. Y. Chen, J. Y. Liu, and G. J. Bailey, "Behaviour of the low-latitude ionosphere-plasmasphere system at long deep solar minimum," *Indian Journal of Radio and Space Physics*, **41**, April 2012, pp. 89-97, https://irsl.ss.ncu.edu.tw/media/paper/2012159_Uke5VAN.pdf.

10. N. Balan, C. Y. Chen, P. K. Rajesh, J. Y. Liu, and G. J. Bailey, "Modeling and observations of the low latitude ionosphere-plasmasphere system at long deep solar minimum," *Journal of Geophysical Research*, **117**, 8, August 2012, pp. A08316, doi: 10.1029/2012JA017846.

11. H. Luhr, and C. Xiong, "IRI-2007 model overestimates electron density during the 23/24 solar minimum," *Geophysical Research Letters*, **37**, 23, December 2010, pp. L23101, doi: 10.1029/2010GL045430.

12. L. Liu, H. Le, Y. Chen, M. He, W. Wan, and X. Yue, "Features of the middle- and low-latitude ionosphere during solar minimum as revealed from COSMIC radio occultation measurements," *Journal of Geophysical Research*, **116**, 9, September 2011, pp. A09307, doi: 10.1029/2011JA016691.

13. E. A. Araujo-Pradere, R. Redmon, M. Fedrizzi, R. Viereck, and T. J. Fuller-Rowell, "Some Characteristics of the Ionospheric Behavior During the Solar Cycle 23–24 Minimum," *Solar physics*, **274**, April 2011, pp. 439–456, doi:10.1007/s11207-011-9728-3.

14. R. Pfaff, D. Rowland, H. Freudenreich, K. Bromund, G. Le, M. Acuña, J. Klenzing, C. Liebrecht, S. Martin, W. J. Burke, N. C. Maynard, D. E. Hunton, P. A. Roddy, J. O. Ballenthin, and G. R. Wilson, "Observations of DC Electric Fields in the Low Latitude Ionosphere and Their Variations with Local Time, Longitude, and Plasma Density during Extreme Solar Minimum," *Journal of Geophysical Research*, **115**, 12, December 2010, pp. A12324, doi:10.1029/2010JA016023.

15. R. A. Stoneback, R. A., R. A. Heelis, A. G. Burrell, W. R. Coley, B. G. Fejer, and E. Pacheco, "Observations of quiet time vertical drift in the equatorial ionosphere during the solar minimum period of 2009," *Journal of Geophysical Research*, **116**, 12, December 2011, pp. A12327, doi:10.1029/2011JA016712.

16. H. Liu, and S. Watanabe, "Observations of quiet time vertical drift in the equatorial ionosphere during the solar minimum period of 2009," *Journal of Geophysical Research*, **113**, 8, August 2008, pp. A08315, doi: 10.1029/2008JA013027.

17. L. Scherliess, D.C. Thompson, and R.W. Schunk, "Longitudinal variability of low-latitude total electron content: tidal influences," *Journal of Geophysical Research*, **113**, 1, January 2008, pp. A01311, doi: 10.1029/2007JA012480.

18. H. Kil, E.R. Talaat, S.J. Oh, L.J. Paxton, S.L. England, and S.Y. Su, "Wave structures of the plasma density and vertical ExB drift in low latitude F region," *Journal of Geophysical Research*, **113**, 9, September 2008, pp. A09312, doi: 10.1029/2008JA013106.

19. P.K. Bhuyan, and R. Hazarika, "GPS TEC near the crest of the EIA at 95^0E during the ascending half of solar cycle 24 and comparison with IRI simulations," *Advances in Space research*, **52**, 7, October 2013, pp. 1247–1260, doi: 10.1016/j.asr.2013.06.029

20. B.R. Kalita, R. Hazarika, G. Kakoti, P. K. Bhuyan, D. Chakrabarty,G. K. Seemala, K. Wang, S. Sharma, T. Yokoyama, P. Supnithi, T. Komolmis, C. Y. Yatini, M. Le Huy1, and P. Roy, "Conjugate hemisphere ionospheric response to the St. Patrick's Day storms of 2013 and 2015 in the 100°E longitude sector," *Journal of Geophysical Research*, **121**, 11, October 2016, pp. 11364–11390, doi: 10.1002/2016JA023119.

21. G.K. Seemala, and C.E.Valladares, "Statistics of total electron content depletions observed over the South American continent for the year 2008," *Radio Science*, **46**, 5, October 2011, pp. RS5019, doi: 10.1029/2011RS004722.

22. D. Bilitza, D. Altadill, V. Truhlik, V. Shubin, I. Galkin, B. Reinisch, and X. Huang, "International Reference Ionosphere 2016: From ionospheric climate to real-time weather predictions," *Space Weather*, **15**, 2, February 2017, pp. 418-429, doi:10.1002/2016SW001593.

23. T. L. Gulyaeva, F. Arikan, and I. Stanislawska, "Inter-hemispheric imaging of the ionosphere with the upgraded IRI-Plas model during the space weather storms," *Earth Planets Space*, **63**, December 2011, pp. 929–939, doi: 10.5047/eps.2011.04.007.

24. Y. K. Chasovitin, T. L. Gulyaeva, M. G. Deminov, and S. E. Ivanova, "Russian Standard Model of the Ionosphere (SMI)," *in Proceedings of 2nd COST251 Workshop*, 1998, pp. 161–172, doi:10.1002/2016SW001593.

25. T. L. Gulyaeva, F. Arikan, Hernandez-Pajares, and I. Stanislawska, "GIM-TEC adaptive ionospheric weather assessment and forecast system," *Journal of Atmospheric and Solar-Terrestrial Physics,* **102**, September 2013, pp. 329–340, doi: 10.1016/j.jastp.2013.06.011.

26. J. D. Huba, G. Joyce, and J. A. Fedder, "Sami2 is Another Model of the Ionosphere (SAMI2): A new low-latitude ionosphere model," *Journal of Geophysical Research,* **105**, 10, October 2000, pp. 23035–23053, doi: 10.1029/2000JA000035.

27. J. D. Huba, G. Joyce, and J. A. Fedder, "The formation of an electron hole in the topside equatorial ionosphere *Geophysical Research Letters,* **27**, 2, January 2000, pp. 181–184, doi: 10.1029/1999GL010735.

28. T. L. Gulyaeva, F. Arikan, Hernandez-Pajares, and I. Stanislawska, "GIM-TEC adaptive ionospheric weather assessment and forecast system," *Journal of Atmospheric and Solar-Terrestrial Physics,* **102**, September 2013, pp. 329–340, doi: 10.1016/j.jastp.2013.06.011.

29. J. D. Huba, G. Joyce, and J. A. Fedder, "Sami2 is Another Model of the Ionosphere (SAMI2): A new low-latitude ionosphere model," *Journal of Geophysical Research,* **105**, 10, October 2000, pp. 23035–23053, doi: 10.1029/2000JA000035.

30. J. D. Huba, G. Joyce, and J. A. Fedder, "The formation of an electron hole in the topside equatorial ionosphere *Geophysical Research Letters,* **27**, 2, January 2000, pp. 181–184, doi: 10.1029/1999GL010735.

31. J. Klenzing, A.G. Burrell, R.A. Heelis, J.D Huba, R. Pfaff, and F. Simoes, "Exploring the role of ionosphere drivers during the extrem solar minimum of 2008," *Annales Geophysics,* **31**, December 2013, pp. 2147–2156, doi:10.5194/angeo-31-2147-2013.

32. P. G. Richards, J. A. Fennelly, and D. G. Torr, "EUVAC: A solar EUV Flux Model for aeronomic calculations," *Journal of Geophysical Research,* **99**, 5, May 1994, pp. 8981–8992, doi:10.1029/94JA00518.

33. J. L. Lean, J. T. Emmert, J. M. Picone and R. R. Meier, "Global and regional trends in ionospheric total electron content," *Journal of Geophysical Research,* **116**, 2, February 2011, pp. A00H04, doi:10.1029/2010JA016378.

34. C. Y. Huang, S. H. Delay, P. A. Roddy, E. K. Sutton and R. Stoneback, "Longitudinal structures in the equatorial ionosphere during deep solar minimum," *Journal of Atmospheric and Solar-Terrestrial Physics,* **90-91**, 2, December 2012, pp. 156–163, doi: 10.1016/j.jastp.2012.04.012.

35. S. L. England , S. Maus, T. J. Immel and S. B. Mende, "Longitudinal variation of the E-region electric fields caused by atmospheric tides," *Geophysical Research Letters,* **33**, 21, November 2006, pp. L21105, doi: 10.1029/2006GL027465.